The AAPS Journal, Vol. 11, No. 2, June 2009 (© 2009)
DOI: 10.1208/s12248-009-9111-6

Research Article

Theme: Towards Integrated ADME Prediction: Past, Present, and Future Directions
Guest Editors: Lawrence X. Yu, Steven C. Sutton, and Michael B. Bolger

Simulations of the Nonlinear Dose Dependence for Substrates of Influx and Efflux Transporters in the Human Intestine

Michael B. Bolger,[1,2,3] Viera Lukacova,[1] and Walter S. Woltosz[1]

Received 7 January 2009; accepted 20 April 2009; published online 12 May 2009

Abstract. The purpose of this study was to develop simulation and modeling methods for the evaluation of pharmacokinetics when intestinal influx and efflux transporters are involved in gastrointestinal absorption. The advanced compartmental absorption and transit (ACAT) model as part of the computer program GastroPlus™ was used to simulate the absorption and pharmacokinetics of valacyclovir, gabapentin, and talinolol. Each of these drugs is a substrate for an influx or efflux transporter and all show nonlinear dose dependence within the normal therapeutic range. These simulations incorporated the experimentally derived gastrointestinal distributions of transporter expression levels for oligopeptide transporters PepT1 and HPT1 (valacyclovir); System L-amino acid transporter LAT2 and organic cation transporter OCTN1 (gabapentin); and organic anion transporter (OATP1A2) and P-glycoprotein (talinolol). By assuming a uniform distribution of oligopeptide transporter and by application of the *in vitro* K_m value for valacyclovir, the simulations accurately reproduced the experimental nonlinear dose dependence. For gabapentin, LAT2 distribution produced simulation results that were much more accurate than OCTN1 distributions. For talinolol, an influx transporter distribution for OATP1A2 and the efflux transporter P-glycoprotein distributed with increasing expression in the distal small intestine produced the best results. The physiological characteristics of the small and large intestines used in the ACAT model were able to accurately account for the positional and temporal changes in concentration and carrier-mediated transport of the three drugs included in this study. The ACAT model reproduced the nonlinear dose dependence for each of these drugs.

KEY WORDS: expression; intestine; saturation; simulation; transporter.

INTRODUCTION

Many drug molecules are substrates for carrier-mediated intestinal transport, and there have been many reviews of drug interaction with the ATP-binding cassette (ABC) superfamily and the solute carrier (SLC) superfamily of transporters in the literature (1–7). At the apical membrane of enterocytes, the ABC transporters primarily result in efflux, while the SLC transporters facilitate influx. On the basolateral membrane, some members of the SLC family exhibit bidirectional transport. All of these transporters are thought to have evolved in order to facilitate absorption of hydrophilic nutrients that could not be well absorbed by a passive mechanism and to protect the animal or human from potentially poisonous hydrophobic xenobiotic molecules. Classification of drug molecules on the basis of metabolism and transport resulted in the development of a Biopharmaceutics Drug Disposition Classification System where highly metabolized (generally hydrophobic) molecules are assigned to class II and hydrophilic molecules that are excreted renally and in many cases are substrates for endogenous transporters are assigned to class III (8).

Transporters also play an important role in distribution and elimination. Vectorial drug transport from blood to bile through the liver has been studied and modeled using simulation methods (9–11). These models included transporters in the basolateral membrane and in the cannilicular membrane. Finally, the study of drug interaction with transporters using simulation methods can help address a topic of growing concern to the US FDA: drug–drug interactions mediated by molecules competing for transporter sites (12,13).

Modeling and simulation have played a significant role in our understanding of the dynamics of drug interaction with intestinal enzymes and transporters (14–20). The first application of Michaelis–Menten kinetics to model absorption was applied to 500-mg oral administration of cefatrizine (21) in which a one-compartment model for comparison of absorption by first-order, zero-order, or Michaelis–Menten kinetics was applied. Those authors concluded that the Michaelis–Menten simulations provided a statistically significant improvement in the optimized fit to *in vivo* data with a K_m value of 2.4 μM. Sinko

[1] Simulations Plus, Inc., 42505 10th Street West, Lancaster, California 93534, USA.
[2] 6 6th Street, Petaluma, California 94952, USA.
[3] To whom correspondence should be addressed. (e-mail: bolger@simulations-plus.com)

and Amidon (22) used *in situ* rat single-pass perfusion to measure the K_m for cefatrizine at 600 μM. This value of K_m was applied to accurately simulate the nonlinear dose dependence of three doses of cefatrizine using a model based on seven small intestine compartments (14).

Critical to accurate simulation of drug interactions with intestinal transporters is the knowledge of the regional distributions of transporter expression in the intestinal tract. Several groups have now used reverse-transcriptase polymerase chain reaction (RT-PCR) to measure the regional expression of messenger RNA (mRNA) specific for intestinal transporters (23–26). These studies are the foundation of our ability to simulate the nonlinear dose dependence for substrates of intestinal transporters. Our previous work with talinolol and the advanced compartmental absorption and transit (ACAT) simulations described here represent the first demonstrations of gastrointestinal simulation for saturable processes involving influx and efflux transporters using experimental regional distributions of transporters. It should be noted that very few experimental distributions of transporter expression have been verified by quantitation of protein rather than mRNA. For this study, the human distribution of P-glycoprotein is the only transporter for which protein expression has been measured. Although the authors are aware that mRNA levels do not always quantitatively predict protein expression levels, in the absence of additional data, we have assumed that mRNA levels reasonably well reflect the local expression of transporters and can be used for these simulations.

For this study, two substrates for influx transport (valacycovir and gabapentin) and one substrate for both influx and efflux transporters (talinolol) were selected. The substrates for influx transporters exhibit decreasing bioavailability with increasing dose due to saturation of PepT1, HPT1, or LAT2. Talinolol is a substrate for the influx transporter Oatp1a5 in rat small intestine, but the K_m value is 2 mM, and so it is not likely to saturate at normal therapeutic doses (27). OATP1A2 is the closest human equivalent to rat Oatp1a5 (28), so equal K_m values for rat and human transporters were assumed.[1] Talinolol is also a substrate for an efflux transporter and exhibits greater than proportional increases in area under the curve (AUC) with increasing dose due to saturation of the ATP-binding cassette transporter P-glycoprotein (P-gp). Three groups have reported the intestinal distribution of PepT1 (23–25), one group has reported the distribution of HPT1 (24), two groups have reported the distribution of P-gp (26,23), one group has reported the distribution of OCTN1 (25), one group has reported the distribution of LAT2 (29), and one group has reported the distribution of OATP1A2 (25). Each of these regional distributions was employed in GastroPlus simulations to find out which of them would best explain the clinical data for the nonlinear dose dependence of absorption for the different transporter substrates. Another objective was to determine if the K_m values from *in vitro* studies could be used directly in the ACAT simulations. This test provided a strong validation of the physiological accuracy of the ACAT model.

Oligopeptide transporters are known to be expressed preferentially in the proximal intestine (duodenum, jejunum, and ileum), and both valacyclovir and amoxicillin have been shown to be substrates (30). One group reported very high levels of expression of PepT1 in the duodenum (approximately fivefold higher than jejunum) (24). Another group reported the highest expression of PepT1 in the ileum (23), and a third group reported a uniform distribution of PepT1 throughout the small intestine (25). Another oligopeptide transporter, HPT1, is also reported to be uniformly distributed in the small intestine (24). This study answers the question: What is the impact on simulation results using these three distributions?

Gabapentin has been reported to be a substrate for two different intestinal transporters (31,32). At the apical membrane of the enterocytes, OCTN1 is the predominant transporter, while at the basolateral membrane of the enterocyte, LAT2 is the primary transporter. Simulation methodology answers the question: Which of these two transporters best accounts for the shape of the Cp *vs*. time profile and the nonlinear *in vivo* dose dependence?

Talinolol is likely to be a substrate for an influx transporter (OATP1A2) and has also been shown to be a substrate for an efflux transporter (P-gp) both on the apical membrane of the enterocytes (33). Here, we ask the question: How does the distribution of OATP1A2 and P-gp affect the results and interplay between dose and regional transport?

METHODS

Simulations

Simulations were run on a standard Toshiba Satellite laptop computer with 2.0 Gb of RAM and 1.8-GHz dual core Intel processor using ver. 6.0.0020 of the GastroPlus software.

ACAT Model

The ACAT model in GastroPlus was used to simulate the nonlinear absorption of five oral doses (100 to 1,000 mg) of valacyclovir, four oral doses (400 to 1,600 mg) of gabapentin, and four oral doses of talinolol (25 to 400 mg). The ACAT model compartment volumes, transit times, radii, pH, and lengths are listed in Table I.

The relative physiological distribution of influx transporters PepT1, HPT1, OCTN1, LAT2, OATP1A2, and P-gp are listed in Table II. In all cases except for the P-gp protein expression measured by Mouly *et al*., the regional distributions represent mRNA expressions quantified by RT-PCR Northern blot analysis [(23), #2877] (24–26). GastroPlus simulations of the nonlinear dose dependence of Cp *vs*. time profiles for the three studied drugs were compared using these distributions.

Valacyclovir

Valacyclovir is a polar ampholyte prodrug of acyclovir with high solubility and low passive permeability. Its absorption is completely dependent on oligopeptide transporters

[1] Note: Added in proof. Talinolol has been demonstrated to be a substrate for both human OATP1A2 and OATP2B1 in Xenopus oocytes (Ikumi Tamai, personal communication).

Table I. ACAT Model Compartment Parameters for Fasted Human Physiology

Compartment	Volume (mL)[a]	Radius (cm)	Length (cm)	Transit time (h)	pH
Stomach	47[b]	9.67	28.3	0.25	1.3
Duodenum	42	1.53	14.1	0.26	6.0
Jejunum1	154	1.45	58.4	0.93	6.2
Jejunum2	122	1.29	58.4	0.74	6.4
Ileum1	94	1.13	58.4	0.58	6.6
Ileum2	71	0.98	58.4	0.42	6.9
Ileum3	49	0.82	58.4	0.29	7.4
Caecum	47	3.39	13.2	4.19	6.4
Asc. Colon	50	2.41	27.6	12.57	6.8

[a] Volume of the small intestinal compartments was calculated as $\pi r^2 L \times 0.4$. This represents the volume of fluid in the compartment volume as 40% of the geometrical volume of the compartment
[b] Volume of the stomach was set at 47 mL in the fasted state and was independent of the length and radius

(34,30,35). Table III lists the biopharmaceutical properties and references used in the simulation of the nonlinear dose dependence.

Dissociation Constants

Valacyclovir is ionized throughout the pH range in the gastrointestinal tract. The molecule has three major sites for ionization (36). Valacyclovir has high solubility throughout the physiological pH range (1.7–7.5), and our simulations predict it to be rapidly dissolved without precipitation for all five oral doses.

Passive Permeability

The effective permeability of valacyclovir measured in a steady-state uptake procedure in rat was found to be concentration-dependent with a K_m=1.2 mM (30). The permeability of valacyclovir in Caco-2 cells (1.70×10^{-6} cm/s) that were transiently transfected with PepT1 (Caco-2/hPepT1 cells) was found to be stereoselective for the L-amino acid and was tenfold more permeable than acyclovir (37). In addition, the permeability of valacyclovir was five times greater in Caco-2/hPepT1 cells than in Caco-2 cells that were not transfected with PepT1. This implies that the passive transcellular permeability of valacyclovir should be quite low (0.34×10^{-6} cm/s) compared with highly permeable molecules like propranolol (26.6×10^{-6} cm/s) (38). Using this ratio and the experimental human jejunal effective permeability (hPeff) of propranolol (2.72×10^{-4} cm/s), the passive transcellular hPeff for valacyclovir was estimated to be 0.03×10^{-4} cm/s and was used for all simulations.

IV Pharmacokinetics

Valacyclovir is rapidly hydrolyzed both in the lumen of the intestine and in the cytoplasm of the enterocyte. Virtually no valacyclovir (<1%) is detected in the systemic circulation following oral administration (39). Therefore, the dose in our simulations was adjusted to reflect the milligram quantity of acyclovir that would be found in an equivalent molar quantity of valacyclovir. Pharmacokinetic (PK) parameters were fitted to i.v. plasma concentration–time data using the PKPlus™ module in GastroPlus. We used the fitted values of clearance (CL), volume of central compartment (V_c), and peripheral compartment distribution rate constants (k_{12}, k_{21}), along with the reported value for plasma protein binding (fup), as a starting point for optimization of the influx V_{max} for oligopeptide transporter in GastroPlus across all five doses. Plasma concentration *vs.* time data for acyclovir in humans were obtained from Soul-Lawton *et al.* (40) for intravenous bolus (350-mg infusion of acyclovir over 1 h) and from Weller *et al.* (39) for oral doses (100-, 250-, 500-, 750-, and 1,000-mg doses of valacyclovir).

Table II. RT-PCR Northern Blot of Transporter Expressions (relative to Ileum as 1.0) Used in the GastroPlus Simulations

Compartment	PepT1[a]	PepT1[b]	PepT1[c]	HPT1[b]	P-gp[a]	P-gp[d]	OCTN1[c]	LAT2[e]	OATP 1A2[c]
Duodenum	0.72	8.42	1.02	1.06	0.16	0.70	0.42	0.74	0.07
Jejunum1	0.92	1.48	1.01	1.17	1.23	0.84	0.71	4.57	0.07
Jejunum2	0.92	1.48	1.01	1.17	1.23	0.94	0.71	4.57	0.07
Ileum1	1.00	1.00	1.00	1.00	1.00	1.00	1.00	1.00	1.00
Ileum2	1.00	1.00	1.00	1.00	1.00	1.09	1.00	1.00	1.00
Ileum3	1.00	1.00	1.00	1.00	1.00	1.07	1.00	1.00	1.00
Caecum	0.02	0	0.04	1.36	0.36	1.3	0.34	0	0.13
Asc. Colon	0.02	0	0.04	1.70	0.36	1.3	0.34	0	0.17

[a] From (23)
[b] From (24)
[c] From (25)
[d] From (26)
[e] From (29)

Table III. Key Biopharmaceutical and Pharmacokinetic Properties of Valacyclovir

Property	Value	Reference
S+Log P	−0.95	Estimated by ADMET Predictor (Simulations Plus, Inc.)
Aqueous solubility (mg/mL)	174	Merck index
Passive jejunal permeability (cm/s)	0.03×10^{-4}	Estimated from Caco-2 Papp (37)
pK_a values	Acid=9.4 Base1=1.9 Base2=7.4	(45)
Clearance (L h^{-1} kg^{-1})	0.211	Fitted from 5 mg/kg i.v. infusion data
V_c (L/kg)	0.216	Fitted from 5 mg/kg i.v. infusion data
K_{12} (h^{-1})	1.31	Fitted from 5 mg/kg iv infusion data
K_{21} (h^{-1})	0.87	Fitted from 5 mg/kg iv infusion data
First pass extraction (%)	34	Fixed across all five oral doses
Lumenal degradation (%/h) at pH=5	2.69	(30)
Lumenal degradation (%/h) at pH=6.5	40.4	(30)
Lumenal degradation (%/h) at pH=7.5	80.6	(30)
In situ transporter K_m (μM)	1200	(30)

Lumenal Degradation

The reported mean absolute bioavailability of valacyclovir is 54%, but it is known to be dose-dependent. Presystemic hydrolysis of valacyclovir to acyclovir occurs both in the lumen of the intestine and in the cytoplasm of the enterocytes. Hydrolysis in the lumen of the intestine can be treated as first pass extraction because the acyclovir that is formed in the lumen of the intestine will not be well absorbed and has been found in feces (40). GastroPlus calculated the rate of lumenal hydrolysis of valacyclovir as a function of pH from a table of observed degradation rates *vs*. pH (30). Finally, we applied a fixed first pass extraction of 34% in addition to the lumenal degradation to account for additional presystemic loss of acyclovir in the enterocytes and liver. The fraction unbound in plasma for acyclovir was taken to be 85% (41).

Simulation of Five Oral Doses

The nonlinear dose dependence for five PO doses of valacyclovir has been reported in healthy human volunteers [(39), #1234]. The subjects in this study fasted from 8 h before until 4 h after receiving the dose. Each volunteer was fed a standardized meal at 4 and 10 h after each dose. The ability of the GastroPlus simulations to match the observed Cp–time data were compared using three published distributions of intestinal PepT1 and one distribution of HPT1. For each oligopeptide distribution, the *in vitro* K_m was used and the V_{max} for the transporter was optimized simultaneously across all five doses. The value of the square of the coefficient of determination (R^2) and the root mean square error (RMSE) of the simulated *vs*. observed plasma concentration *vs*. time (Cp *vs*. time) profile were determined for each distribution of oligopeptide transporter.

Gabapentin

Gabapentin is a hydrophilic amino acid with high solubility and low passive permeability. It is known to be a substrate for OCTN1 (*SLC22A4*, Na^+-independent) in the apical membrane of the enterocytes (31). It is also a substrate of the System L (SLC7) family of amino acid transporters; LAT1 light chain (with 4F2hc heavy chain, Na^+-independent family) in the apical membranes of brain, placenta, and tumors (32,42) and LAT2 light chain (with 4F2hc heavy chain, Na^+-independent family) in the basolateral membrane of the enterocytes (42). Its absorption is entirely dependent on active transporters (43). LAT1 and LAT2 are amino acid exchangers with 1:1 stoichiometry: The transporter transfers one amino acid out of the cell and at the same time another amino acid molecule is transported into the cell (44). Table IV lists the biopharmaceutical properties and references used in the physiologically based pharmacokinetic (PBPK) simulations of the nonlinear dose dependence. Although the K_m for the intracellular gabapentin binding site

Table IV. Key Biopharmaceutical and Pharmacokinetic Properties of Gabapentin used in the PBPK Simulations

Property	Value	Reference
Log$D_{7.4}$	−1.1	(47)
Solubility (in water mg/mL)	100	(45)
Passive jejunal permeability (cm/s)	0.04×10^{-4}	Calculated by ADMET Predictor (43) (not detectable)
pK_a values	Acid=3.68 Base=10.7	(43)
Plasma unbound (%)	>97	(31)
Renal clearance (L h^{-1} kg^{-1})	0.086	Set as GFR × fup for 41 year-old female
V_{ss} (L/kg)	0.611	V_{ss} calc. (46)
First pass extraction (%)	0	Not metabolized
LAT2 transporter K_m (μM)	5811	Fitted across five oral doses

Table V. Key Biopharmaceutical and Pharmacokinetic Properties of Talinolol

Property	Value	Reference
Log$D_{7.4}$	1.08	(59)
Solubility (at pH 7.4 mg/mL)	1.23	(59)
Jejunal permeability (cm/s)[a]	1.29×10^{-4}	(27)
pK_a values	Base=9.43	(59)
Plasma unbound (%)	45	(60)
Clearance (L h^{-1} kg^{-1})	0.38	Fitted from 30 mg i.v. data (61)
V_c (L/kg)	1.21	Fitted from 30 mg i.v. data (61)
k_{12} (h^{-1})	1.37	Fitted from 30 mg i.v. data (61)
k_{21} (h^{-1})	0.98	Fitted from 30 mg i.v. data (61)
k_{13} (h^{-1})	0.52	Fitted from 30 mg i.v. data (61)
k_{31} (h^{-1})	0.14	Fitted from 30 mg i.v. data (61)
First pass extraction (%)	0	Not metabolized
P-gp transporter K_m (μM)	6.3	Optimized across four oral doses
OATP1A2 K_m (μM)	2000	(27)

[a] The permeability was measured in rat (1.29×10^{-4} cm/s) and converted to human permeability (4.06×10^{-4} cm/s) by considering the correlation between rat and human jejunal effective permeability (62)

of LAT2 has not been determined, the intracellular sites for other neutral amino acids are in the millimolar range (44). For this study, we fitted the apparent K_m for the intracellular basolateral transporter binding site of gabapentin based on the regional distribution of the LAT2 transporter.

Dissociation Constants

Gabapentin is ionized in the stomach and is zwitterionic at pH values from 6 to 8 throughout the small and large intestines. The molecule has two major sites for ionization: a carboxylic acid (pK_a=3.68) and a primary amine (pK_a=10.7) (43). Gabapentin has high solubility throughout the physiological pH range (1.7–7.5) (45) and is predicted to be rapidly dissolved without precipitation using all four oral doses in our simulations.

Passive Permeability

The effective permeability of gabapentin was measured using the *in situ* single-pass intestinal perfusion technique in fasted rats (43). The contribution of both passive and carrier-mediated transport was determined. The passive permeability was not significantly different than zero and the active component was saturable and concentration-dependent. Rather than run the gabapentin simulation in GastroPlus without any passive permeability, we decided to use the estimated human jejunal permeability from ADMET Predictor (S+Peff). The estimated value of S+Peff was 0.04×10^{-4} cm/s, and this value was used for all gabapentin simulations.

Physiologically Based Pharmacokinetics

Physiologically-based PK was used with a calculated value of V_{ss} using the method of Berezhkovskiy (46) along with the reported value for plasma protein binding (fup=98%) (31) and log$D_{7.4}$=−1.1 (47) as a starting point for optimization/fitting in GastroPlus across all five doses. Plasma concentration *vs*. time data in humans for one 400-mg PO solution dose (48) and four tablet PO doses from 400 mg tid up to 1,600 mg tid (49) were obtained. The reported mean absolute bioavailability (F) of the 400-mg PO IR tablet dose was 49% and the F is reported to decrease to 29% at steady-state following a 1,600-mg tid dose (49). The fraction unbound in plasma used in the simulations was 98% (31).

The pharmacokinetics of gabapentin following a single 400-mg solution dose (48) and the nonlinear dose dependence of escalating capsule doses from 400 to 1,600 mg tid (49) has been reported. In addition, a recent study compared 600 mg of Neurontin™ tid to an 1,800-mg gastric-retentive extended release formulation (50). The published distributions of intestinal OCTN1 (25) and intestinal LAT2 (29) were used for the GastroPlus simulations of gabapentin. The RMSE of the simulated *vs*. observed plasma concentration *vs*. time (Cp *vs*. time) profiles were determined for each distribution of transporter.

Talinolol

We have previously reported simulations of the nonlinear dose dependence, pharmacokinetics, and pharmacodynamics for talinolol. This study will compare the accuracy of those simulations with more recently reported distributions of P-gp (15). The methods for GastroPlus simulations and biopharmaceutical properties for talinolol were reported previously (15) and are repeated briefly here. Key biopharmaceutical properties used in the simulations of talinolol are shown in Table V.

Talinolol is a moderately hydrophobic weak base that is 99.9% cationic at pH=6.5 and has moderate human jejunal permeability. Talinolol also has four instances of a type II pattern of electron donors which has been suggested to be

Table VI. Percent Absorbed and Bioavailable for Oral Valacyclovir Using Englund PepT1 Distribution

Dose (mg)	Fa%	F%	F% without active transport
100	81.7	53.8	1.5
250	76.7	50.5	1.5
500	70.9	46.7	1.5
750	66.7	43.8	1.5
1,000	63.5	41.7	1.5

Table VII. Comparison of Simulation Results for Valacyclovir Using Four Different Oligopeptide Distributions

Dose (mg)	E-PepT1[a] *F*% (R^2, RMSE)	M-PepT1[b] *F*% (R^2, RMSE)	H-PepT1[c] *F*% (R^2, RMSE)	H-HPT1[c] *F*% (R^2, RMSE)
100	53.8 (0.88, 0.096)	54.5 (0.84, 0.12)	50.3 (0.69, 0.18)	54.3 (0.86, 0.11)
250	50.5 (0.93, 0.16)	51.0 (0.91, 0.18)	44.2 (0.74, 0.32)	50.9 (0.92, 0.17)
500	46.7 (0.96, 0.19	46.9 (0.95, 0.23)	37.1 (0.67, 0.56)	47.1 (0.95, 0.21)
750	43.8 (0.93, 0.36)	43.9 (0.92, 0.39)	32.1 (0.69, 0.62)	44.3 (0.92, 0.38)
1,000	41.7 (0.96, 0.31)	41.7 (0.96, 0.31)	28.7 (0.60, 0.93)	42.3 (0.96, 0.33)
Ave. R^2	0.93	0.92	0.68	0.92

[a] From (23)
[b] From (25)
[c] From (24)

commonly found in substrates of P-gp (51). It has been suggested that molecules with moderate permeability have the greatest potential to be influenced by the efflux transporters (19). Molecules with higher permeability are able to diffuse rapidly across the cell membrane and avoid binding to the P-gp substrate binding site. Molecules with lower permeability tend to be too polar for partitioning into the membrane and achieving access to the P-gp binding site. Also, since talinolol is a substrate for the rat Oatp1a5 and most likely a substrate for the human influx transporter OATP1A2, intracellular enterocyte concentrations of talinolol might be higher than if the only influx mechanism was passive, resulting in a greater influence of P-gp *in vivo*.

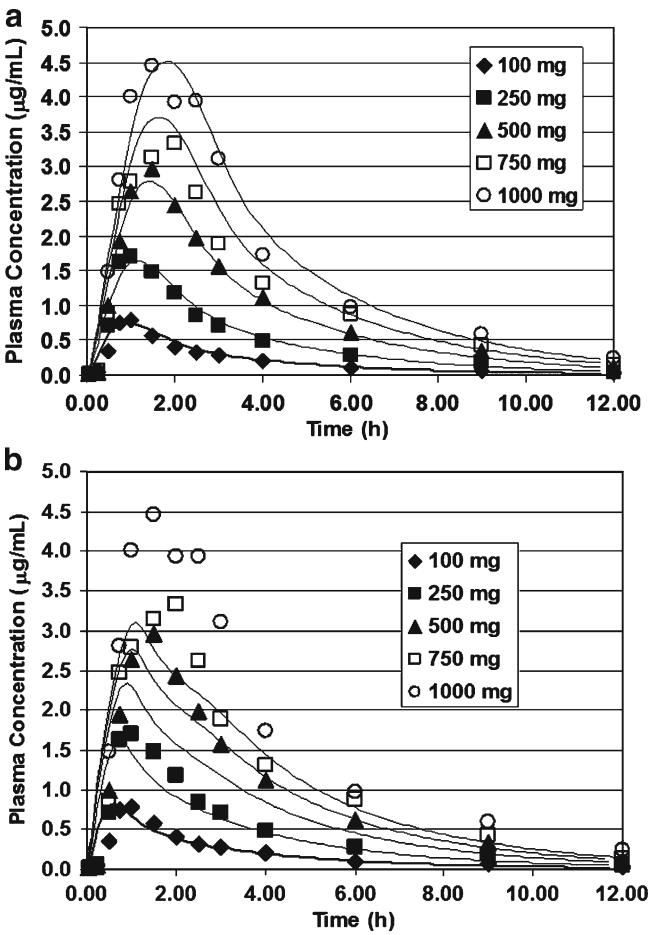

Fig. 1. Valacyclovir simulations using experimental distributions of PepT1. Oral doses of valacyclovir (100 to 1,000 mg) administered to volunteers at risk for developing Herpes simplex virus (*HSV*) (39). **a** Using the Englund distribution of PepT1 (23). **b** Using the Herrera–Ruiz distribution of Pept1

RESULTS

Valacyclovir

Valacyclovir is a polar ampholyte with high solubility and low passive permeability. Table VI shows the simulated values for percent absorbed (Fa%) and bioavailability (*F*%) across all five doses with and without influx transport due to oligopeptide transporters in the apical membrane of the small intestine. The Englund distribution of PepT1 was used to simulate these results. It is clear that the absorption is completely dependent on influx transport since the fraction absorbed in the absence of such transporters is <2%. Also, it can be seen that the fraction absorbed and bioavailability decreases with increasing dose due to saturation of the influx transporter.

Table VII is a comparison of the quality of the fit for each dose when four different oligopeptide distributions were used in the simulations. It is apparent that the approximately uniform distributions of oligopeptide transporter, as observed for the Englund PepT1, Meier PepT1, and Herrera–Ruiz

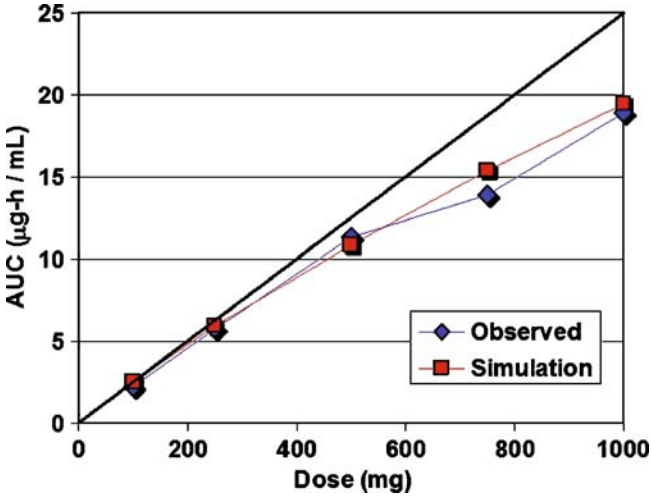

Fig. 2. Observed and simulated AUC for each dose. The observed AUC was calculated using trapezoidal integration of the observed Cp *vs*. time profiles. Simulated AUCs represent the area under the curve for the simulated lines. The line of identity (*black line*) would occur in the absence of nonlinear dose dependence

Table VIII. Percent Bioavailable for Oral Gabapentin Using LAT2 and OCTN1 Distributions

Dose (mg)	Dave LAT2 *F*% (R^2, RMSE)	Meier OCTN1 *F*% (R^2, RMSE)	*F*% without active transport
400	54.8 (0.89, 0.31)	70.5 (0.25, 0.77)	5.9
800	46.5 (0.81, 0.62)	57.0 (0.36, 1.1)	5.9
1,200	40.7 (0.90, 0.49)	48.0 (0.31, 1.2)	5.9
1,600	36.4 (0.83, 0.83)	41.8 (0.29, 1.5)	5.9
Ave. R^2	0.86	0.24	5.9

HPT1 distributions, give similar quality of fit and accuracy of the nonlinear dose dependence, while the Herrera–Ruiz PepT1 distribution gives a very poor fit.

Figure 1a, b shows a comparison of the fits for all five doses using the Englund and the Herrera–Ruiz PepT1 distributions. Figure 2 is a comparison of the observed AUC and the simulated AUC as function of dose for simulations employing the Englund distribution. Simulations employing any other one of the uniform distributions of oligopeptide transporter produce similar results. The Herrera–Ruiz PepT1 distribution has approximately fivefold higher expression in the duodenum and fits the data nicely at the lower doses (100 and 250 mg). However, at the higher doses, saturation of the duodenal transporter results in lower C_{max} values than observed in the clinical data.

Gabapentin

Gabapentin is a polar zwitterion with high solubility and low passive permeability. Table VIII shows the simulated values for bioavailability (*F*%) across all four doses with and without active transport due to LAT2 (29) or OCTN1 (25) transporters of the small intestine. It is clear that the absorption is almost completely dependent on active transport since the fraction absorbed in the absence of transporters is <6%. Also, it can be seen that regardless which transporter distribution is used, the bioavailability decreases with increasing dose due to saturation of the influx transporter.

Figure 3a, b shows the results of nonlinear simulations using two different distributions of the intestinal transporter. The murine LAT2 distribution is highest in the jejunum and four times lower in the ileum with none in the colon and results in a rapid rise in systemic concentration as seen in Fig. 3a. In GastroPlus, if we use the human OCTN1 distribution which is expressed throughout the small and large intestine, we see a delayed T_{max} due to colonic absorption that is absent in the LAT2 distribution.

The improved quality of fit suggests that LAT2 is the rate-determining transport barrier for gabapentin. Although LAT2 is mainly distributed on the basolateral membrane of the enterocyte, we chose to simplify the simulations and allow a direct comparison of the OCTN1 and LAT2 distributions by applying equations with both transporters in the apical membrane of the enterocyte. Our simulations suggest that the LAT2 distribution best explains the shape of the Cp *vs.* time (Fig. 3a) so that LAT2 transport is the more likely rate-limiting process in absorption of gabapentin.

Talinolol

Talinolol is a hydrophobic secondary amine that is a good substrate for P-gp and shows a nonlinear dose dependence in the normal therapeutic range of doses (52). Previously, we used GastroPlus to model the nonlinear dose dependence of talinolol and we linked the resulting simulations to a pharmacodynamic model of the heart rate response (15). At that time, only one publication by Mouly and Paine (26) had described the intestinal distribution of P-gp, which concluded from Western blot gels of P-gp protein that the expression increased from the proximal to distal regions of the small intestine. Englund *et al.* have since

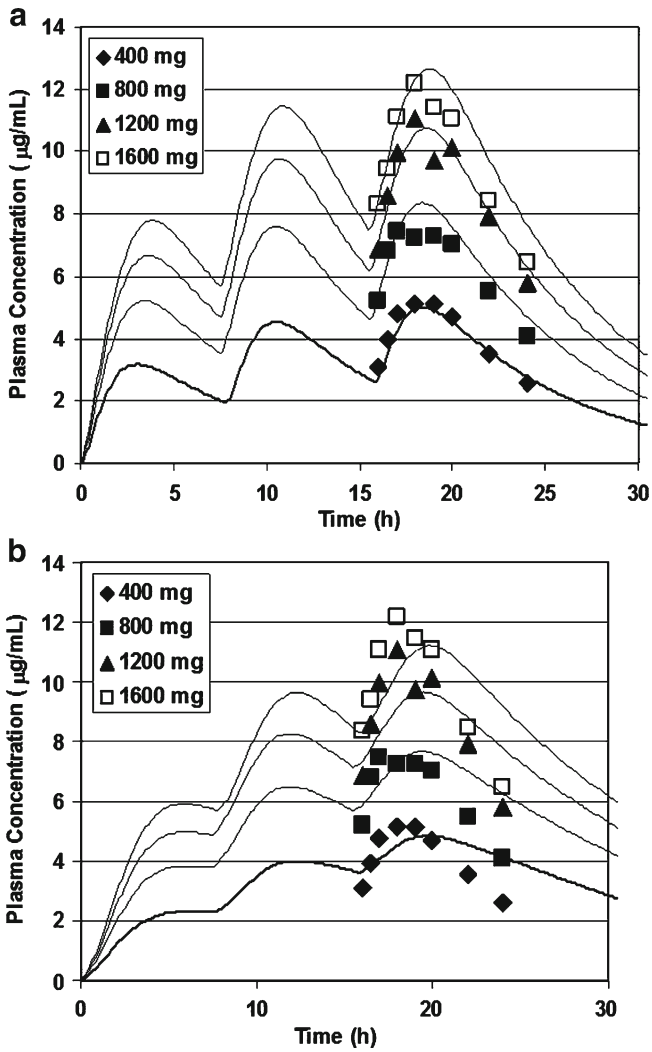

Fig. 3. **a** Gabapentin simulations using experimental distributions of expression. Gabapentin was administered to epileptic patients at doses from 400 to 1,600 mg tid. Cp *vs.* time data was collected after the third dose. **a** Using the murine LAT2 distribution of transport protein expression (29). **b** Using the human OCTN1 distribution of transport protein expression (25)

Table IX. Percent Bioavailable for Oral Talinolol using OATP1A2 and P-pg Distributions

Dose (mg)	Mouly P-pg Distribution $F\%$ (R^2, RMSE)	Englund P-pg Distribution $F\%$ (R^2, RMSE)
25	65.4 (0.79, 5.6)	73.5 (0.76, 4.3)
50	73.2 (0.82, 11.0)	83.9 (0.51, 15.2)
100	82.7 (0.76, 29.2)	91.2 (0.63, 30.1)
400	94.2 (0.89, 104)	97.4 (0.74, 143)
Ave. R^2	0.82	0.66

published the intestinal distribution of P-gp mRNA and the expression pattern is reversed, with higher expression in the proximal small intestine (see Table II). Tang *et al.* (53,54) studied Yucatan micropig and determined that the mRNA distribution was higher in the proximal SI, but P-gp protein increased distally from the duodenum to the ileum. We decided to create a GastroPlus model using the Englund distribution to compare with the Mouly distribution that increases aborally. A recent publication reported that talinolol is also a substrate for Oatp1a5 in rats (27). The closest human transporter to Oatp1a5 is OATP1A2, so we added this transporter to our simulations of the nonlinear dose dependence assuming the K_m would be the same as for rat.

Table IX presents the simulated bioavailability results for talinolol using both the Mouly and the Englund P-gp distributions, clearly showing better prediction with the Mouly distribution. Figure 4a, b shows predicted Cp–time and AUC *vs.* dose for talinolol using the Mouly P-gp distribution in the simulations. It can be seen that regardless of which transporter distribution is used, bioavailability increases with increasing dose due to saturation of the efflux transporter. Figure 4a, b shows predicted Cp–time and AUC *vs.* dose for talinolol using the Mouly P-gp distribution.

DISCUSSION

The application of mechanistic simulations to study the absorption of drugs that are substrates for intestinal transporters reveals several insights that might not be available from *in vitro* studies of transporter–substrate interactions. By integrating all of the available data on physicochemical and biopharmaceutical properties, simulations provide results that predict both the passive and active components of absorption and they explain the shape of the Cp *vs.* time profile on the basis of the regional distribution of transporters.

Valacyclovir

In vitro studies of inhibition of valacyclovir permeability suggested that multiple transporters were involved (30). More recent studies using gene chip analysis of transporter expression in patients being treated with valacyclovir have shown high correlation between HPT1 expression and AUC for valacyclovir (35). Our simulations show that a uniform distribution of a saturable transporter best explains the observed nonlinear dose dependence for valacyclovir. However, it is not possible to prove that only one transporter is responsible for valacyclovir absorption. Both PepT1 and HP1 have been shown to transport valacyclovir *in vitro*, but the literature presents conflicting data for the exact regional distribution of these transporters. Our present study suggests that a uniform distribution of an oligopeptide transporter best explains the shape and nonlinear dose dependence of the Cp *vs.* time profile. *In vivo*, the regulation of oligopeptide transporter expression is more complex than the picture that

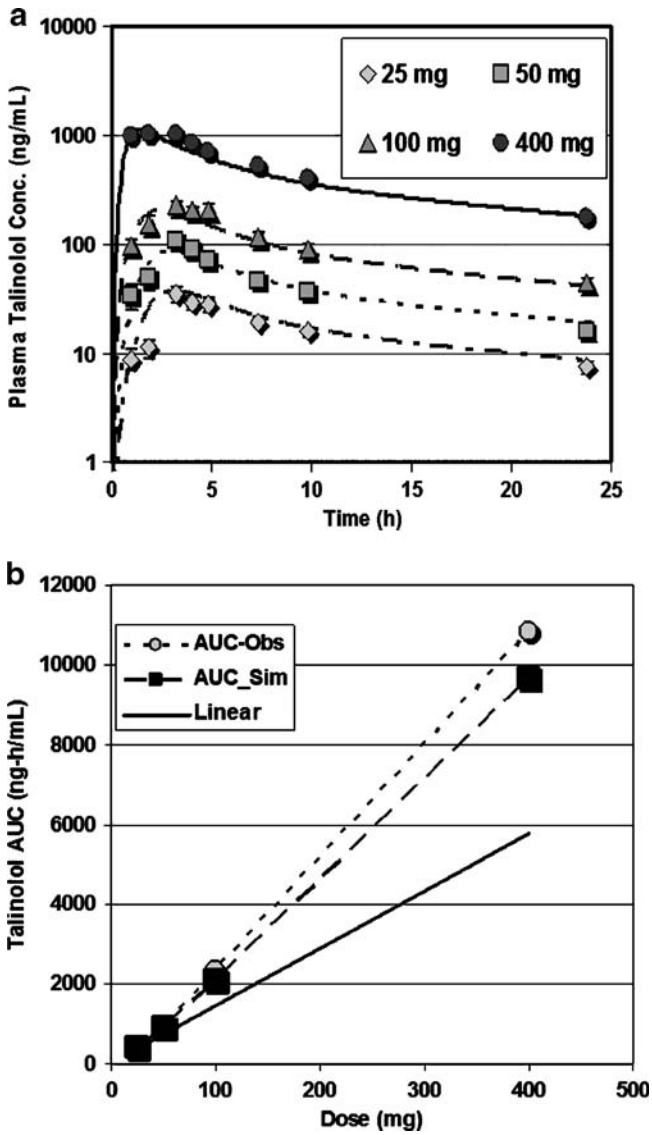

Fig. 4. Talinolol simulations using Mouly distribution of P-gp. Oral doses of talinolol (25 to 400 mg) were administered to 12 healthy subjects (52). **a** Simulated and observed of Cp *vs.* time profiles for four oral doses. **b** The observed AUC was calculated using trapezoidal integration of the observed Cp *vs.* time profiles. Simulated AUCs represent the area under the curve for the simulated lines. The line of identity (*black line*) would occur in the absence of nonlinear dose dependence

emerges from these simulations. Naruhashi *et al*. (55) demonstrated in rats that starvation induced the expression of PepT1 in the proximal small intestine. In fed rats, the absolute expression was one fifth to one sixth of the levels in the starved condition, and the expression was higher in the distal small intestine. Thus, it is likely that *in vivo*, the regional distribution of oligopeptide transporters varies depending on the nutritional state.

Gabapentin

Our understanding of gabapentin absorption and amino acid transport in general is still evolving. The System L-amino acid transporters LAT1 and LAT2 are known to exchange large neutral amino acids across the apical and basolateral membranes of epithelial cells in the intestine, brain, placenta, tumors, and kidney (56,44). The intracellular binding sites for these two transporters have been shown to have lower affinity for substrates (K_m in the high millimolar range) than the extracellular sites (K_m in the low millimolar range), but the substrate selectivity of both sites is similar (44). The role of LAT1 and LAT2 is most likely equilibration of the amino acid distribution across the two membranes, whereas other unidirectional transporters determine the actual net amino acid flux (44). The recent discovery that OCTN1, located on the apical membrane of the enterocytes, transports gabapentin into the cell, along with the existence of low affinity intracellular LAT2 sites, suggests that high intracellular concentrations of gabapentin are required for saturation. Our simulation results support this conclusion and suggest that gabapentin crosses the apical membrane of the enterocyte rapidly and subsequent transfer to the portal vein is regulated by LAT2.

Talinolol

Our previous simulation studies of talinolol provided a good model for explaining the nonlinear dose dependence of interaction with P-gp (15), but did not include the recent discovery that it is also a substrate for an influx transporter in rats (Oatp1a5) (27). In that study, we used a distribution of P-pg based on the results from Mouly and Paine (26). Here, we compared the Mouly distribution of P-gp (increasing in the distal SI) to the Englund distribution (highest P-gp expression in the jejunum) and found again that the Mouly distribution best explains the observed *in vivo* nonlinear dose dependence. In this study, we added the apical influx transporter OATP1A2 (a close human homolog to rat Oatp1a5) into the simulation. This resulted in a better fit (later T_{max}) to the shape of the *in vivo* talinolol Cp *vs*. time profile due to the relatively high expression of OATP1A2 in the ileum.

Using Caco-2 cell monolayers, Troutman and Thakker (57) found that the apparent K_m for P-gp-mediated efflux of digoxin was greater than sixfold larger in the absorptive *vs*. the secretory direction. For structurally diverse P-gp substrates (acebutolol, colchicine, digoxin, etoposide, methylprednisolone, prednisolone, quinidine, and talinolol), the apparent K_m was approximately three to eightfold greater in the absorptive *vs*. the secretory transport direction. Korjamo *et al*. (58) studied the passive permeability and active efflux of quinidine and digoxin in Caco-2 cell monolayers with variable degrees of P-gp expression. They found that as the P-gp expression increased; the apparent K_m and V_{max} determined from the apical-to-basolateral direction also increased. In addition, the apparent K_m value showed a strong inverse relationship to the passive permeability. In contrast, the apparent V_{max} value was maximum at intermediate passive permeability. If P-gp expression is high, intracellular concentrations will be lower than the extracellular concentrations due to faster efflux, resulting in the need for higher extracellular concentrations to achieve half-maximal saturation of the intracellular transporter binding site. This would also account for K_m values that are lower when measured from the basolateral-to-apical direction than vice versa. Our simulation results consistently show that the true intracellular K_m required to reproduce the experimental nonlinear dose dependence for talinolol (6.3 μM) is lower than the K_m measured *in vitro* from the apical-to-basolateral direction (414 μM) and lower than the K_m measured *in vitro* from the basolateral-to-apical direction (103 μM) (57). Thus, an accurate cellular simulation program may be helpful in converting *in vitro* experimental results for efflux transporter K_m values to values that can be used for *in silico* prediction of the *in vivo* consequences during development of drugs that are substrates for efflux transporters.

OCTN1 has low affinity for talinolol (K_m=2,000 μM) and would not be saturated even at high lumenal concentrations (1,100 μM for 400-mg dose in duodenum). However, talinolol affinity for P-gp is much higher than for OCTN1, so even when considering the low simulated intracellular enterocyte concentration, saturation does occur and so a simulation incorporating Michaelis–Menten kinetics accurately represents the nonlinear dose dependence for talinolol.

CONCLUSIONS

This study demonstrates the ability of the ACAT model within GastroPlus to simulate the *in vivo* absorption and pharmacokinetics for substrates of influx and efflux transporters in the small intestine. In some cases (e.g., valacyclovir), the value of K_m measured *in situ* or *in vitro* can be used directly to accurately reproduce a nonlinear dose dependence. When the experimental value of K_m is not known (e.g., gabapentin), simulation results help to indicate which transporter(s) is(are) primarily responsible for carrier-mediated absorption. For substrates of efflux transporters in the small intestine, *in vitro* values of K_m determined by measuring transepithelial transport in the apical-to-basolateral or basolateral-to-apical directions must be corrected to represent the half-maximal concentration for substrate binding to transporter sites inside the enterocyte.

REFERENCES

1. Custodio JM, Wu CY, Benet LZ. Predicting drug disposition, absorption, elimination, transporter interplay and the role of food on drug absorption. Adv Drug Deliv Rev. 2008;60(6):717–33.
2. Nakamura T, Yamamori M, Sakaeda T. Pharmacogenetics of intestinal absorption. Curr Drug Deliv. 2008;5(3):153–69.
3. Steffansen B, Nielsen CU, Brodin B, Eriksson AH, Andersen R, Frokjaer S. Intestinal solute carriers: an overview of trends and strategies for improving oral drug absorption. Eur J Pharm Sci. 2004;21(1):3–16.

4. Sai Y, Tsuji A. Transporter-mediated drug delivery: recent progress and experimental approaches. Drug Discov Today 2004;9(16):712–20.
5. Mizuno N, Niwa T, Yotsumoto Y, Sugiyama Y. Impact of drug transporter studies on drug discovery and development. Pharmacol Rev. 2003;55(3):425–61.
6. Tsuji A. Transporter-mediated drug interactions. Drug Metab Pharmacokinet. 2002;17(4):253–74.
7. Sadee W, Drubbisch V, Amidon GL. Biology of membrane transport proteins. Pharm Res. 1995;12(12):1823–37.
8. Wu CY, Benet LZ. Predicting drug disposition via application of BCS: transport/absorption/elimination interplay and development of a biopharmaceutics drug disposition classification system. Pharm Res. 2005;22(1):11–23.
9. Ito K, Suzuki H, Horie T, Sugiyama Y. Apical/basolateral surface expression of drug transporters and its role in vectorial drug transport. Pharm Res. 2005;22(10):1559–77.
10. Shitara Y, Sugiyama Y. Pharmacokinetic and pharmacodynamic alterations of 3-hydroxy-3-methylglutaryl coenzyme A (HMG-CoA) reductase inhibitors: drug–drug interactions and interindividual differences in transporter and metabolic enzyme functions. Pharmacol Ther. 2006;112(1):71–105.
11. Liu L, Cui Y, Chung AY, Shitara Y, Sugiyama Y, Keppler D, et al. Vectorial transport of enalapril by Oatp1a1/Mrp2 and OATP1B1 and OATP1B3/MRP2 in rat and human livers. J Pharmacol Exp Ther. 2006;318(1):395–402.
12. Shitara Y, Horie T, Sugiyama Y. Transporters as a determinant of drug clearance and tissue distribution. Eur J Pharm Sci. 2006;27(5):425–46.
13. US FDA. Draft guidance for industry: drug interaction studies—study design, data analysis, and implications for dosing and labeling, U.S.D.o.H.a.H. services, editor; 2006. Rockville: Center for Drug Evaluation and Research.
14. Yu LX, Amidon GL. Saturable small intestinal drug absorption in humans: modeling and interpretation of cefatrizine data. Eur J Pharm Biopharm. 1998;45(2):199–203.
15. Tubic M, Wagner D, Spahn-Langguth H, Bolger MB, Langguth P. *In silico* modeling of non-linear drug absorption for the P-gp substrate talinolol and of consequences for the resulting pharmacodynamic effect. Pharm Res. 2006;23(8):1712–20.
16. Bolger MB, Haworth IS, Yeung AK, Ann D, von Grafenstein H, Hamm-Alvarez S, *et al*. Structure, function, and molecular modeling approaches to the study of the intestinal dipeptide transporter PepT1. J Pharm Sci. 1998;87(11):1286–91.
17. Agoram B, Woltosz WS, Bolger MB. Predicting the impact of physiological and biochemical processes on oral drug bioavailability. Adv Drug Deliv Rev. 2001;50(Suppl 1):S41–67.
18. Gonzalez-Alvarez I, Fernandez-Teruel C, Casabo-Alos VG, Garrigues TM, Polli JE, Ruiz-Garcia A, *et al*. *In situ* kinetic modelling of intestinal efflux in rats: functional characterization of segmental differences and correlation with *in vitro* results. Biopharm Drug Dispos. 2007;28(5):229–39.
19. Kwon H, Lionberger RA, Yu LX. Impact of P-glycoprotein-mediated intestinal efflux kinetics on oral bioavailability of P-glycoprotein substrates. Mol Pharm. 2004;1(6):455–65.
20. Pang KS. Modeling of intestinal drug absorption: roles of transporters and metabolic enzymes. Drug Metab Dispos. 2003;31(12):1507–19.
21. Reigner BG, Couet W, Guedes JP, Fourtillan JB, Tozer TN. Saturable rate of cefatrizine absorption after oral administration to humans. J Pharmacokinet Biopharm. 1990;18(1):17–34.
22. Sinko PJ, Amidon GL. Characterization of the oral absorption of beta-lactam antibiotics. I. Cephalosporins: determination of intrinsic membrane absorption parameters in the rat intestine *in situ*. Pharm Res. 1988;5(10):645–50.
23. Englund G, Rorsman F, Ronnblom A, Karlbom U, Lazorova L, Grasjo J, *et al*. Regional levels of drug transporters along the human intestinal tract: co-expression of ABC and SLC transporters and comparison with Caco-2 cells. Eur J Pharm Sci. 2006;29(3–4):269–77.
24. Herrera-Ruiz D, Wang Q, Gudmundsson OS, Cook TJ, Smith RL, Faria TN, *et al*. Spatial expression patterns of peptide transporters in the human and rat gastrointestinal tracts, Caco-2 *in vitro* cell culture model, and multiple human tissues. AAPS PharmSci. 2001;3(1):E9.
25. Meier Y, Eloranta JJ, Darimont J, Ismair MG, Hiller C, Fried M, *et al*. Regional distribution of solute carrier mRNA expression along the human intestinal tract. Drug Metab Dispos. 2007;35(4):590–4.
26. Mouly S, Paine MF. P-glycoprotein increases from proximal to distal regions of human small intestine. Pharm Res. 2003;20(10):1595–9.
27. Shirasaka Y, Li Y, Shibue Y, Kuraoka E, Spahn-Langguth H, Kato Y, *et al*. Concentration-dependent effect of naringin on intestinal absorption of beta(1)-adrenoceptor antagonist talinolol mediated by P-glycoprotein and organic anion transporting polypeptide (Oatp). Pharm Res 2009;26:560–7.
28. Hagenbuch B, Meier PJ. Organic anion transporting polypeptides of the OATP/SLC21 family: phylogenetic classification as OATP/SLCO superfamily, new nomenclature and molecular/functional properties. Pflugers Arch. 2004;447(5):653–65.
29. Dave MH, Schulz N, Zecevic M, Wagner CA, Verrey F. Expression of heteromeric amino acid transporters along the murine intestine. J Physiol. 2004;558(Pt 2):597–610.
30. Sinko PJ, Balimane PV. Carrier-mediated intestinal absorption of valacyclovir, the l-valyl ester prodrug of acyclovir: 1. Interactions with peptides, organic anions and organic cations in rats. Biopharm Drug Dispos. 1998;19:209–17.
31. Urban TJ, Brown C, Castro RA, Shah N, Mercer R, Huang Y, et al. Effects of genetic variation in the novel organic cation transporter, OCTN1, on the renal clearance of gabapentin. Clin Pharmacol Ther. 2008;83(3):416–21.
32. Uchino H, Kanai Y, Kim do K, Wempe MF, Chairoungdua A, Morimoto E, *et al*. Transport of amino acid-related compounds mediated by L-type amino acid transporter 1 (LAT1): insights into the mechanisms of substrate recognition. Mol Pharmacol. 2002;61(4):729–37.
33. Doppenschmitt S, Spahn-Langguth H, Regardh CG, Langguth P. Role of P-glycoprotein-mediated secretion in absorptive drug permeability: an approach using passive membrane permeability and affinity to P-glycoprotein. J Pharm Sci. 1999;88(10):1067–72.
34. Han H, de Vrueh RL, Rhie JK, Covitz KM, Smith PL, Lee CP, et al. 5′-Amino acid esters of antiviral nucleosides, acyclovir, and AZT are absorbed by the intestinal PEPT1 peptide transporter. Pharm Res. 1998;15(8):1154–9.
35. Landowski CP, Sun D, Foster DR, Menon SS, Barnett JL, Welage LS, *et al*. Gene expression in the human intestine and correlation with oral valacyclovir pharmacokinetic parameters. J Pharmacol Exp Ther. 2003;306(2):778–86.
36. Balimane P, Sinko P. Effect of ionization on the variable uptake of valacyclovir via the human intestinal peptide transporter (hPepT1) in CHO cells. Biopharm Drug Dispos. 2000;21(5):165–74.
37. Han HK, Oh DM, Amidon GL. Cellular uptake mechanism of amino acid ester prodrugs in Caco-2/hPEPT1 cells overexpressing a human peptide transporter. Pharm Res. 1998;15(9):1382–6.
38. Adson A, Burton PS, Raub TJ, Barsuhn CL, Audus KL, Ho NF. Passive diffusion of weak organic electrolytes across Caco-2 cell monolayers: uncoupling the contributions of hydrodynamic, transcellular, and paracellular barriers. J Pharm Sci. 1995;84(10):1197–204.
39. Weller S, Blum MR, Doucette M, Burnette T, Cederberg DM, de Miranda P, *et al*. Pharmacokinetics of the acyclovir pro-drug valaciclovir after escalating single- and multiple-dose administration to normal volunteers. Clin Pharmacol Ther. 1993;54(6):595–605.
40. Soul-Lawton J, Seaber E, On N, Wootton R, Rolan P, Posner J. Absolute bioavailability and metabolic disposition of valaciclovir, the L-valyl ester of acyclovir, following oral administration to humans. Antimicrob Agents Chemother. 1995;39(12):2759–64.
41. MacDougall C, Guglielmo BJ. Pharmacokinetics of valaciclovir. J Antimicrob Chemother. 2004;53(6):899–901.
42. del Amo EM, Urtti A, Yliperttula M. Pharmacokinetic role of L-type amino acid transporters LAT1 and LAT2. Eur J Pharm Sci. 2008;35(3):161–74.
43. Madan J, Chawla G, Arora V, Malik R, Bansal AK. Unbiased membrane permeability parameters for gabapentin using boundary layer approach. AAPS J. 2005;7(1):E224–30.
44. Meier C, Ristic Z, Klauser S, Verrey F. Activation of system L heterodimeric amino acid exchangers by intracellular substrates. EMBO J. 2002;21(4):580–9.

45. Kasim NA, Whitehouse M, Ramachandran C, Bermejo M, Lennernas H, Hussain AS, *et al*. Molecular properties of WHO essential drugs and provisional biopharmaceutical classification. Mol Pharm. 2004;1(1):85–96.
46. Berezhkovskiy LM. Volume of distribution at steady state for a linear pharmacokinetic system with peripheral elimination. J Pharm Sci. 2004;93(6):1628–40.
47. Vollmer KO, von Hodenberg A, Kolle EU. Pharmacokinetics and metabolism of gabapentin in rat, dog and man. Arzneimittelforschung 1986;36(5):830–9.
48. Gidal BE, Radulovic LL, Kruger S, Rutecki P, Pitterle M, Bockbrader HN. Inter- and intra-subject variability in gabapentin absorption and absolute bioavailability. Epilepsy Res. 2000;40 (2–3):123–7.
49. Gidal BE, DeCerce J, Bockbrader HN, Gonzalez J, Kruger S, Pitterle ME, *et al*. Gabapentin bioavailability: effect of dose and frequency of administration in adult patients with epilepsy. Epilepsy Res. 1998;31(2):91–9.
50. Gordi T, Hou E, Kasichayanula S, Berner B. Pharmacokinetics of gabapentin after a single day and at steady state following the administration of gastric-retentive- extended-release and immediate-release tablets: a randomized, open-label, multiple-dose, three-way crossover, exploratory study in healthy subjects. Clin Ther. 2008;30(5):909–16.
51. Seelig A. A general pattern for substrate recognition by P-glycoprotein. Eur J Biochem. 1998;251(1–2):252–61.
52. de Mey C, Schroeter V, Butzer R, Jahn P, Weisser K, Wetterich U, *et al*. Dose–effect and kinetic–dynamic relationships of the beta-adrenoceptor blocking properties of various doses of talinolol in healthy humans. J Cardiovasc Pharmacol. 1995;26(6):879–8.
53. Tang H, Pak Y, Mayersohn M. P-glycoprotein (P-gp) mRNA and protein expression pattern along the small intestine of the Yucatan micropig. AAPS Annual Meeting. 2002. Toronto, Canada.
54. Tang H, Pak Y, Mayersohn M. Protein expression pattern of P-glycoprotein along the gastrointestinal tract of the Yucatan micropig. J Biochem Mol Toxicol. 2004;18(1):18–22.
55. Naruhashi K, Sai Y, Tamai I, Suzuki N, Tsuji A. PepT1 mRNA expression is induced by starvation and its level correlates with absorptive transport of cefadroxil longitudinally in the rat intestine. Pharm Res. 2002;19(10):1417–23.
56. Rossier G, Meier C, Bauch C, Summa V, Sordat B, Verrey F, et al. LAT2, a new basolateral 4F2hc/CD98-associated amino acid transporter of kidney and intestine. J Biol Chem. 1999;274 (49):34948–54.
57. Troutman MD, Thakker DR. Efflux ratio cannot assess P-glycoprotein-mediated attenuation of absorptive transport: asymmetric effect of P-glycoprotein on absorptive and secretory transport across Caco-2 cell monolayers. Pharm Res. 2003;20 (8):1200–9.
58. Korjamo T, Kemilainen H, Heikkinen AT, Monkkonen J. Decrease in intracellular concentration causes the shift in K_m value of efflux pump substrates. Drug Metab Dispos. 2007;35 (9):1574–9.
59. Gramatte T, Oertel R, Terhaag B, Kirch W. Direct demonstration of small intestinal secretion and site-dependent absorption of the beta-blocker talinolol in humans. Clin Pharmacol Ther. 1996;59(5):541–9.
60. Trausch B, Oertel R, Richter K, Gramatte T. The protein binding of talinolol. Pharmazie 1995;50(1):72.
61. Trausch B, Oertel R, Richter K, Gramatte T. Disposition and bioavailability of the beta 1-adrenoceptor antagonist talinolol in man. Biopharm Drug Dispos. 1995;16(5):403–14.
62. Kim JS, Mitchell S, Kijek P, Tsume Y, Hilfinger J, Amidon GL. The suitability of an *in situ* perfusion model for permeability determinations: utility for BCS class I biowaiver requests. Mol Pharm. 2006;3(6):686–94.